Curve Tilting With Nonlinear Model Predictive Control for Enhancing Motion Comfort

Yanggu Zheng, Barys Shyrokau, Tamás Keviczky, *Senior Member, IEEE*, Monzer Al Sakka, and Miguel Dhaens

Abstract—The benefits of automated driving can only be fully realized if the occupants are protected from motion sickness. Active suspensions hold the potential to raise the comfort level in automated passenger vehicles by enabling new functionalities in chassis control. One example is to actively lean the vehicle body toward the center of the corner to counteract the inertial lateral acceleration. Commonly known as curve tilting, the concept is deemed effective in reducing postural disturbance on the occupants and the visual-vestibular conflict when the occupants do not have an external view. We present in this article a nonlinear model predictive control (NMPC) method for the curve tilting functionality. The controller incorporates the nonlinear suspension forces in the prediction model to help achieve high tracking accuracy near the physical limit of the suspension system. The optimization process is accelerated with an explicit initialization method that is based on piecewise-affine (PWA) modeling and offline solution to an alternative optimal control problem (OCP). The controller is able to operate at 20 Hz in a hardware-in-the-loop (HIL) setup. Given sufficient computational resources, we observe a significant reduction in the lateral acceleration sensed by the passenger over a vehicle with passive suspensions, namely, by 46.5%, 25.4%, and 25.4% in the highway, rural, and urban driving scenarios, respectively. The NMPC also outperforms the baseline proportional-integral-derivative (PID) controller by achieving lower tracking error, namely, by 12.9%, 16.4%, and 38.0% in the aforementioned scenarios.

Index Terms—Active suspension, model predictive control, motion comfort, real-time optimization.

I. INTRODUCTION

A. Motivation and Background

AUTOMATED driving is expected to free the human drivers from performing the dynamic driving task, allowing them to engage in secondary activities [1]. Carrying
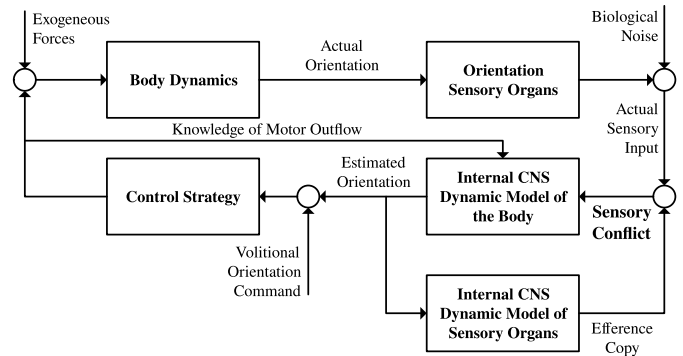
Fig. 1. Observer model of motion sickness according to the sensory conflict theory, adopted from [7].

out productive or recreational activities during daily transit significantly benefits both individual car users and the entire society. However, by taking the eyes off the road, the occupants inside a car are exposed to a higher risk of developing motion sickness [2]. Symptoms of motion sickness, including dizziness, drowsiness, headache, nausea, etc., may harm the occupant's task performance and willingness to perform the task [3]. Apparently, the anticipated benefits cannot be fully realized if motion sickness remains a challenging problem. Hence, the comfort of automated vehicles is receiving more research interest.

Among all forms of motion that a passenger vehicles exhibits, comfort related to the vertical motion has been studied extensively in the past. The suspension system plays an influential role in vertical comfort by filtering out the disturbances in the vertical direction which are mainly introduced by road irregularities. The suspension system fulfills the role by supporting the vehicle body with the properly chosen stiffness and damping parameters. The parameters aim to minimize the transmission of vertical disturbances while taking into account the human body's frequency sensitivity to vibrations. However, optimizing solely for comfort sacrifices safety, as the wheels' contact with the road becomes less stable. This brings up the trade-off problem when the suspension components have only one set of fixed parameters [4]. The introduction of selective, semi-active (continuous damping), and active suspensions allowed the vertical dynamics to adapt to the road condition and the user's preference [5], [6]. Meanwhile, comfort related to the planar motions (i.e., longitudinal, lateral, and yaw) of a vehicle is not well-developed. The control of
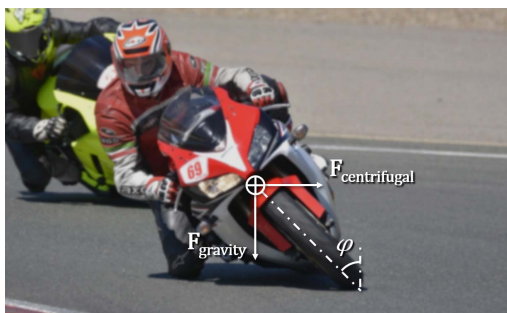
Fig. 2. Balancing centrifugal force with gravity by leaning the body of a single-track vehicle inward.

Fig. 3. Advanced passenger train prototype vehicle undergoing the test for maximum tilting angle [12].

the planar motion has always been considered as the human driver's task before automated driving emerged. According to the visual-vestibular conflict theory [7], motion sickness is induced by the difference between ego-motion sensed from the eyes and the vestibular system (see Fig. 1). When the occupants direct their gaze away from the external surroundings, their eyes perceive the ego-motion as almost static, while the vestibular system still senses the vehicle's movements. In this case, it is potentially effective to minimize the acceleration sensed by the vestibular system. The sensed acceleration can be expressed as the actual centrifugal acceleration introduced by the planar motion multiplied with the transmission ratio from the chassis to the occupant. The former is determined either by the driver in a conventional vehicle or by the motion planning and control algorithms in the case of automated driving. For minimizing the transmission ratio, a concept of actively leaning the vehicle body toward the center of the corner has been implemented and is deemed effective [8]. The concept resembles the cornering behavior of single-track vehicles (e.g., bicycles and motorcycles). By rotating the vehicle body around the roll axis, the gravity is exploited to counteract the centrifugal force (see Fig. 2). Early applications were mainly found on railway vehicles [9] aiming to shorten the travel time without modifying the existing track or sacrificing comfort (see Fig. 3). The function had not become available on passenger vehicles until the 2010s and is only found on high-end passenger vehicles at this moment [10]. The major limiting factors include the complexity and cost of a capable actuator as well as the less predictable motion due to human drivers. In general, road vehicles experience far more dynamic maneuvering than railroad vehicles. The quick changing of the direction and large magnitude of acceleration is highly demanding on the actuator's output, whereas the space allocated for suspension struts is limited. However, the way automated vehicles shape future mobility may see a wider application of active suspensions. On one hand, the concept of shared mobility could lower the customers' sensibility to the manufacturing cost of a single vehicle [11]. More importantly, automated driving allows more potential in the active tilting and other functions enabled by active suspensions.

The state-of-the-art approach of the active curve tilting functionality is based on the preview of road curvature using stereo cameras, combined 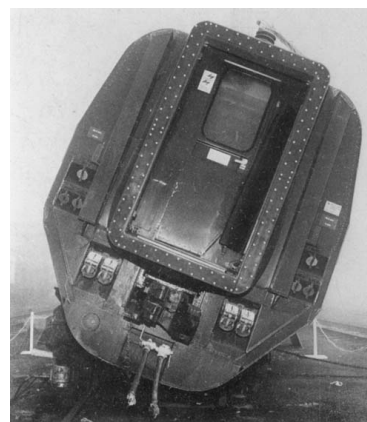with proportional-integral-derivative (PID) control [8]. Previewing curvature alone is not sufficient for predicting the vehicle's planar motion and is a compromised solution for vehicles with little to no automation. With the human driver in the loop, the longitudinal velocity can only be predicted by understanding the driver's intention and the surrounding traffic situation. However, this cannot provide a precise value of the velocity at a certain time ahead. Similarly, the steering action may be presumed by the lane mark and the usage of turning indicators, as implemented in lane-keeping assistance [13]. Nevertheless, such estimation has limited precision, and the actual moment and magnitude of the steering input remain uncertain. With these uncertainties in predicting the steering action, it is difficult to determine the tilting manner of the vehicle body to effectively minimize the lateral disturbance exerted on the occupants. Meanwhile, these uncertainties also harm the control quality of the roll motion. The acceleration (or deceleration) and steering inputs influence the attitude of the vehicle body by causing longitudinal and lateral load transfer, which further exerts additional vertical forces on the suspensions at different locations. Only with reliably predicted planar motion can such forces be estimated in advance and requested from the active suspensions to prevent the vehicle body's attitude from being disturbed. The PID control method, as currently implemented in the automotive industry, exhibits certain disadvantages in this specific application. To maximize the utilization of the stroke length available, the system inevitably operates in the nonlinear range of the spring where linear methods are perceived as less capable. When operating close to certain constraints (e.g., physical limit, actuator's capability) in the system, PID cannot explicitly avoid violations, potentially causing damages to the suspension system in the long term and raising the operational cost of the vehicle.

Alternatively, nonlinear model predictive control (NMPC) is known for its capability of explicitly handling nonlinear system dynamics and constraints. Model predictive control is an optimization-based control method that determines the control input by minimizing a cost function while satisfying certain constraints. Based on the prediction with a model of the system's dynamics throughout a certain prediction

horizon, the cost function accumulates the control effort and the consequential error. By minimizing the cost function, the controller computes the control input that yields an optimal trade-off solution between quality and actuation expenses. Nonlinear MPC is a branch of MPC that allows predicting with nonlinear models and can handle nonlinear constraints if necessary. The underlying numerical optimization problem is more complex than in a linear MPC, where the prediction model and constraints are linear and the cost function is typically quadratic. With few exceptions (e.g., quadratic programming as in a linear MPC), optimization of a nonlinear non-convex cost function requires intensive computation. The main contributor to the computational burden is the complexity of the prediction model that allows the evaluation of the cost function. The evaluation of the cost function is done by simulating the system behavior with the prediction model by means of numerical integration. On top of that, most nonlinear optimization algorithms, including gradient descent, sequential quadratic programming, interior-point method, etc., use the gradient information of the cost function, which is determined numerically if the analytic form of the gradient function is unavailable. The numerical differentiation method further increases the computational cost. Hence, the dimensionality of the input also plays a role. Another contributing factor to the complexity is the non-convexity of the cost function. In practice, it is difficult to verify the convexity of a cost function. Hence, the number of local optima in the function should be considered unknown. Running the aforementioned nonlinear optimization algorithms for one time without proper initialization is at the risk of converging to a local minimum that does not yield a reasonable control input. This problem could be tackled with global optimization heuristics, for example, multistart local search, evolutionary algorithms, and simulated annealing. Such approaches are successful in raising the chance of avoiding local minima but are computationally less efficient. In the case of vehicle dynamics, some studies run NMPC controllers at 20 Hz [14], [15], while linear controllers such as PID and linear quadratic regulator (LQR) can operate at 100 Hz. This makes the aforementioned heuristics that demand heavy computation less desirable in this specific application. Instead, the warm-start technique has been explored to enable real-time implementation of NMPC in vehicle dynamics control. One of the approaches is to initialize the upcoming optimization process using the results of the previous step [16]. The method is effective if the plant is modeled with sufficient accuracy and the magnitude of the disturbance is limited. Only under such conditions, the prediction coincides with the actual behavior of the system and the previous result is still feasible, although not necessarily optimal due to the shift in the prediction horizon. Otherwise, the actual state at the next step may deviate largely from what is predicted and the corresponding control input does not yield a good initial guess anymore. Instead, some studies propose to initialize online optimization with an explicit control law [17]. The explicit control law is computed offline by approximating the optimal solution of the optimization problem with PWA functions. The approach of explicitly initializing the NMPC with an alternative suboptimal controller has been proposed in [18]

and tested with an arbitrary mathematical model. A similar method was implemented in [19], where the explicit controller is computed by solving a comparable hybrid MPC problem offline. The controller aims to stabilize the excessive yaw and lateral motion of a passenger vehicle in case of a rear-end traverse impact. Such approaches effectively move a portion of the computational effort offline and better use the onboard storage resource.

B. Main Contributions of the Study

In this study, we present an NMPC control method for the curve tilting functionality that uses explicit initialization to accelerate the solution process for real-time implementation. The system currently relies on a velocity-dependent curvature preview strategy, which will be replaced in the future by an optimization-based reference generator that cooperates with the motion planner. The main contributions of this study include:

1) The application of NMPC to active suspensions for improving lateral motion comfort. The controller directly incorporates the significant nonlinearities of the suspension system within the prediction model, maximizing the range of operation with high tracking accuracy.
2) A tailored explicit initialization scheme to accelerate the solution process in NMPC. A hybrid model of the quarter-car dynamics is formulated, which approximates the nonlinear suspension forces with PWA functions. The resulting hybrid MPC problem is solved offline to yield a good initial guess to the optimization process in the NMPC after further combining with a disturbance estimator capturing the features of rigid-body dynamics that a quarter-car model cannot.
3) A quantitative evaluation of the impact of active tilting concept on lateral motion comfort. The human body's frequency-dependent sensitivity to lateral disturbance is taken into account, with a focus on the range where motion sickness is provoked the most.
4) An HIL experiment on the feasibility of the real-time implementation of the proposed NMPC controller. The hard real-time setup verifies that given very limited computational resources, the NMPC can return the optimized control input within the required sampling time. With a reduced number of iterations, the NMPC can still maintain a satisfactory level of control performance that is superior to the baseline PID controller, thanks to the explicit initialization scheme.

C. Article Structure

The control method is described in detail in Section II. Section III explains the setup for PC-based and HIL simulations, and the results are presented and discussed in Section IV. Section V summarizes the contribution of the study and indicates future possibilities for further enhancing planar motion comfort in automated vehicles.
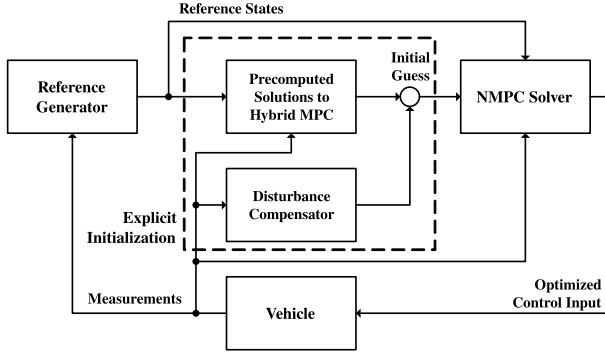
Fig. 4. Schematic drawing of the proposed control approach. The components inside the dashed rectangle belong to the explicit initialization scheme. The NMPC solver takes inputs from the reference generator, the vehicle's onboard sensors, and the output of the initialization to compute an optimal control input to the active suspension actuators.
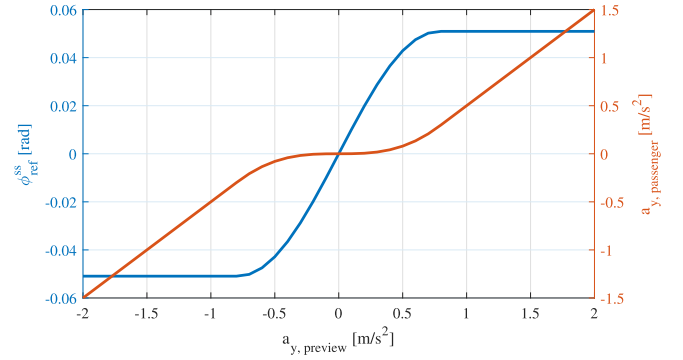

Fig. 5. Reference motion and resultant lateral acceleration sensed by the passenger are plotted versus the previewed lateral acceleration. The previewed lateral acceleration is estimated with the current velocity and the curvature of lane center at 1 s of time ahead.

II. CONTROL APPROACH

This section presents in detail the control approach to the curve tilting application. The control system's main objective is to ensure that the vehicle body's roll angle accurately follows the reference value. The functionality is enabled by active suspension actuators that generate the desired amount of additional vertical force, as commanded by the controller. The force commands are computed under the framework of NMPC. The underlying numerical optimization process is accelerated with a novel explicit initialization method. The control scheme is explained in Fig. 4, and the components will be explained in Sections II-A–II-E.

A. Reference Motion

The desired manner of active roll motion is designed according to comfort-related requirements and physical limitations. The reference roll angle is a function of previewed lateral acceleration on the vehicle chassis at 1 s ahead. The permissible roll angle can reduce the lateral acceleration by at most 0.5 ms^{-2} from what is exerted on the passenger. As the lateral acceleration builds up, it would be undesirable if the roll angle approaches the saturation value with a high velocity. Hence, we adopted a smooth curve shape for the transition (see Fig. 5). A half period of a sinusoid is placed at the origin, connecting two linear sections with constant value

$$\phi_{\text{ref}}^{\text{ss}} = \begin{cases} k_1 \sin(k_2 a_{y,\text{prev}}), & |k_2 a_{y,\text{prev}}| \le \pi/2 \\ k_1, & |k_2 a_{y,\text{prev}}| > \pi/2. \end{cases} \quad (1)$$

The parameter k_1 is set to equal the maximum permissible roll angle $\phi_{\max}$. The parameter k_2 is chosen to meet the following boundary condition:

$$\frac{d\phi_{\text{ref}}^{\text{ss}}}{da_{y,\text{prev}}^{\text{ss}}}\bigg|_{a_{y,\text{prev}}^{\text{ss}}=0} = k_1 k_2 = \frac{1}{g} \quad (2)$$

where g is the gravitational acceleration. This equation expresses the requirement that the slope of the tangent line of the curve at the origin should result in zero lateral acceleration to be sensed by the passenger. It ensures that the minor lateral disturbances are fully compensated for. In addition to the smooth steady-state reference curve, we further applied a low-pass filter on the previewed acceleration, to generate feasible and comfortable reference motion even when the curvature changes abruptly. The filter is defined as

$$a_{y,\text{prev}}(s) = \frac{\omega_n^2}{s^2 + 2\zeta\omega_n s + \omega_n^2} a_{y,\text{prev}}^{\text{ss}}(s) \quad (3)$$

where ω_n and ζ are the natural frequency and the damping coefficient of the filter, respectively. A second-order filter is chosen such that the roll acceleration is bounded and the roll velocity is continuous. The filter exhibits an over-damped behavior (i.e., $\zeta > 1$), which eliminates overshoot and residual oscillations in the reference motion.

B. Prediction Model

The motion regimes of interest include the vehicle body's roll, pitch, and heave, noted by ϕ, θ, and z, respectively. They must be modeled as a whole as these motions interact with each other through the rigid vehicle body. The equations of motion are as follows [20]:

$$I_{xx}\ddot{\phi} = (F_{z,\text{FL}} + F_{z,\text{RL}} - F_{z,\text{FR}} - F_{z,\text{RR}})B/2 \\ - m_{\text{spr}}a_y(h_{\text{cg}} - h_{\text{cr}}) - (I_{zz} - I_{yy})\dot{\theta}\dot{\psi}$$
$$I_{yy}\ddot{\theta} = (F_{z,\text{RL}} + F_{z,\text{RR}})L_{\text{R}} - (F_{z,\text{FL}} + F_{z,\text{FR}})L_{\text{F}} \\ - m_{\text{spr}}a_x(h_{\text{cg}} - h_{\text{cp}}) + (I_{xx} - I_{zz})\dot{\psi}\dot{\phi}$$
$$m_{\text{spr}}\ddot{z} = F_{z,\text{FL}} + F_{z,\text{FR}} + F_{z,\text{RL}} + F_{z,\text{RR}} \quad (4)$$

where h_{cg} is the static height of the center of gravity, and h_{cp} and h_{cr} stand for the static heights of the instant centers of pitch and roll rotations, respectively. The longitudinal distances from the center of gravity of the sprung mass m_{spr} to the front and rear axle are denoted by L_{F} and L_{R}, respectively, whereas the track width of the vehicle is represented by B. The vertical force at each wheel $F_{z,*}$ (where $* \in \{\text{FL, FR, RL, RR}\}$ stands for wheel locations) is a function of the motion states plus the control input from the active suspension actuator $F_{\text{act},*}$

$$F_{z,*} = f_*(\phi, \dot{\phi}, \theta, \dot{\theta}, z, \dot{z}) + F_{\text{act},*}. \quad (5)$$

The planar motions (i.e., longitudinal, lateral, and yaw) are excluded as they are governed by either a human driver or

the motion planning and control on an automated vehicle. Still, the planar motions have a strong influence on these modeled motions. The inertial acceleration causes load transfer in the longitudinal and lateral directions, exerting additional pitch and yaw moments on the vehicle body. The yaw motion is coupled with pitch and roll according to the rotational dynamics of a rigid body governed by Euler's equations.

Suspension forces are the key characteristics to describe in the prediction model. The common approach to suspension control assumes constant spring stiffness and damping coefficient, to obtain a linear model [21], [22]. Since we aim to maximize the utilization of wheel travel for the tilting, the suspension is stretched or compressed to an extent that the linear approximation is no longer valid. On one hand, the kinematics of the suspension system is constrained by its geometry, which is optimized for a linear relationship around the neutral position. As the wheel moves farther away from the neutral position, the control arms rotate largely that the validity of the small-angle approximation no longer holds. Consequently, the compression or stretching of the spring and damper is not proportional to the wheel displacement. In addition, the forces on the spring and damper are not proportional to their displacement or velocity, either. In practice, the spring has a stiffness that gradually increases when compressed, which together with the buffer block protects the components from physical damage due to excessive wheel movements. Meanwhile, the dampers usually exhibit degressive characteristics (i.e., the force-to-velocity ratio decreases as the velocity increases) which prevent the hydraulic cylinder from over-pressurization. Besides, the damper generates less force in the compression stroke than in the stretching stroke. This is mainly done for minimizing the transmission of road disturbance in case an upward impact exerted on the wheel (e.g., when driving over speed bumps or debris), which is more frequently experienced [23]. These nonlinearities can be captured at once by determining the function of force-to-displacement and force-to-velocity relationships. The relevant data can be obtained from the simulation model.

C. Optimal Control Problem

The MPC determines the control input by solving an optimal control problem (OCP) at each time step. An optimal control input sequence of finite length is calculated by minimizing a cost function and the first input in the sequence is forwarded to the controlled system. The OCP is formulated as

$$
\begin{aligned}
\min_{\boldsymbol{u}} \quad & J_{\mathrm{NMPC}}(\boldsymbol{u}) \\
\text{s.t.} \quad & \boldsymbol{u}_{\mathbf{min}} \leq \boldsymbol{u} \leq \boldsymbol{u}_{\mathbf{max}}.
\end{aligned} \tag{6}
$$

The cost function J reflects the priorities of the state tracking errors and control efforts and focuses on a finite horizon from the current moment. In this study, we use a quadratic cost function integrated through the prediction horizon

$$
J = \int_{t_0}^{t_0+t_\mathrm{p}} \left((\boldsymbol{x_t} - \boldsymbol{x}_{\mathrm{ref}})^T \boldsymbol{Q}(\boldsymbol{x_t} - \boldsymbol{x}_{\mathrm{ref}}) + \boldsymbol{u_t}^T \boldsymbol{R}\boldsymbol{u_t} \right) dt \tag{7}
$$

TABLE I
WEIGHTING PARAMETERS OF THE NMPC

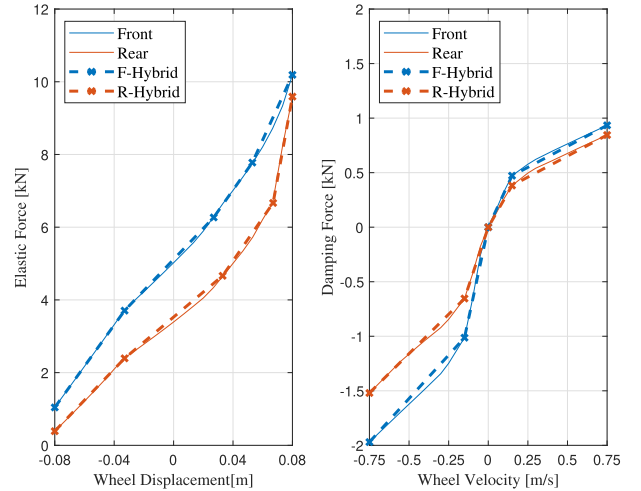| Variable	Unit	Weight
Roll angle	rad	12
Roll rate	rad/s	0.4
Pitch angle	rad	2
Pitch rate	rad/s	0.1
Heave	m	2
Heave rate	m/s	0.1
Actuation force	kN	0.0001

Fig. 6. Suspension force characteristics according to the actual multibody model and the hybrid model for quarter-car dynamics.

where the states, reference states, and inputs are defined as

$$
\begin{aligned}
\boldsymbol{x} &= \left(\phi, \dot{\phi}, \theta, \dot{\theta}, z, \dot{z} \right)^T \\
\boldsymbol{x}_{\mathrm{ref}} &= (\phi_{\mathrm{ref}}, 0, 0, 0, 0, 0)^T \\
\boldsymbol{u_t} &= \left(F_{\mathrm{act,FL}}, F_{\mathrm{act,FR}}, F_{\mathrm{act,RL}}, F_{\mathrm{act,RR}} \right)^T.
\end{aligned} \tag{8}
$$

The cost function is evaluated by means of numerical integration with an Euler step of 50 ms. The control input is fixed through the prediction horizon t_p, i.e., the number of decision variables is 4. The inputs are bounded within the capability of the actuators. Due to the limited information available for predicting the vehicle's planar motion, the exogenous disturbances are assumed constant through the prediction horizon of 0.4 s. The assumption may not be valid for more dynamic situations and could be improved when combined with a motion planner. Minimizing the aforementioned cost function results in an optimal control input that ensures that the reference roll angle is tracked with a minimal error while the influence of the active suspension forces on the pitch (θ and $\dot{\theta}$) and heave (z and $\dot{z}$) motions and the control efforts are kept reasonably low. The values of the weighting parameters are presented in Table I.

D. Explicit Initialization

The numerical optimization process for solving the OCP described above is accelerated with an explicit initialization technique. A hybrid MPC is developed for this purpose. By approximating the nonlinear dynamics with multiple
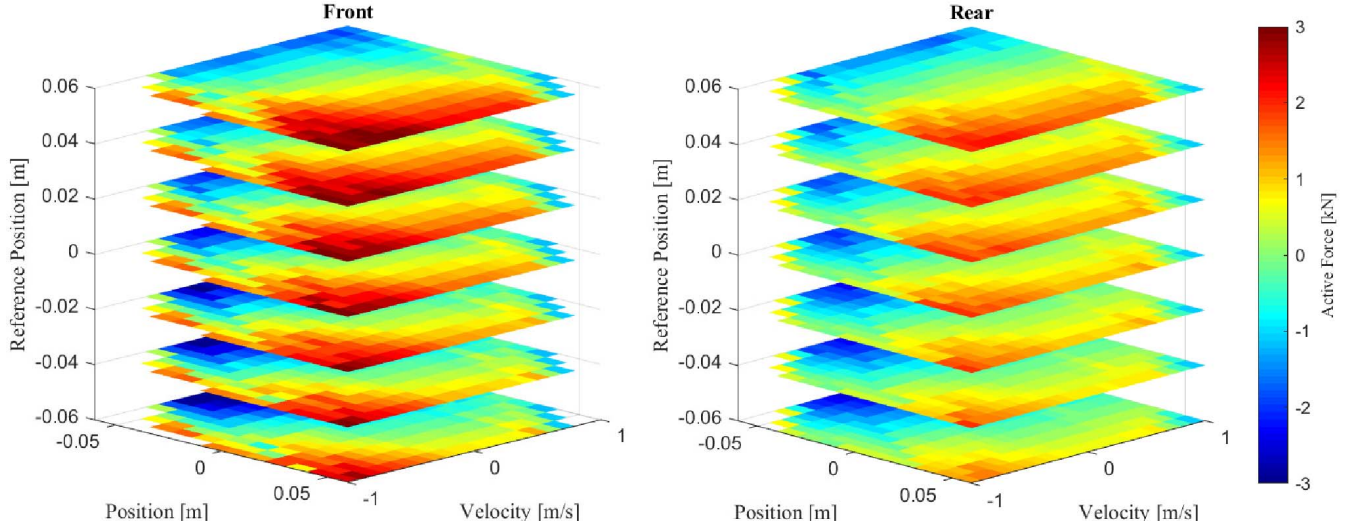
Fig. 7. Slices of the 3-D lookup table for the purpose of explicitly initializing the optimization problem in NMPC.

linear modes under a piecewise affine (PWA) formulation, we formulate the OCP as a mixed-integer quadratic programming (MIQP) problem that can be solved efficiently [25]. Given finite modes and prediction steps, the MIQP problem contains finite binary and continuous variables. It is therefore possible to solve the problem in finite time by naive enumeration of all combinations of the binary variables. The branch-and-bound algorithm only has to do so in the worst case [26]. This feature allows the MIQP problem to be solved with guaranteed global optimality given sufficient computational effort, which is not a problem for offline preparation. Nevertheless, the formulation of a hybrid model of the roll, pitch, and heave motion is complex due to a large number of modes. To overcome this, we divide the whole vehicle body into four separate sprung masses, each suspended above the corresponding wheel. Such dynamics are described with a quarter-car model as

$$
\begin{bmatrix} z_{*,k+1} \\ \dot{z}_{*,k+1} \end{bmatrix} = A_{*,j} \begin{bmatrix} z_{*,k} \\ \dot{z}_{*,k} \end{bmatrix} + B_{*,j} F_{\text{act}, *,k} + f_{*,j}
$$
$$
\begin{bmatrix} z_{*,j,lb} \\ \dot{z}_{*,j,lb} \end{bmatrix} \leq \begin{bmatrix} z_k \\ \dot{z}_k \end{bmatrix} \leq \begin{bmatrix} z_{*,j,ub} \\ \dot{z}_{*,j,ub} \end{bmatrix}
\tag{9}
$$

where j denotes the mode that the system operates in at step k. For each mode j, a corresponding set of A, B, and f is defined based on the PWA approximation of the suspension forces. As Fig. 6 shows, the forces on the front and rear springs and dampers are each divided into four sectors. Given the independence between the spring and the damper, the hybrid quarter-car model contains 16 modes. The decision is based on the fact that most hydraulic dampers on passenger vehicles have four operating modes, namely, the slow bump, fast bump, slow rebound, and fast rebound. For sake of convenience, we also divide the spring characteristics into four pieces. In the hybrid model, the dynamics of the unsprung mass, including the tire, wheel, and wheel hub, are neglected because of the high modal frequency (100 Hz according to [27]) as a result of the high stiffness-to-mass ratio. The sampling frequency of the

MPC, 20 Hz in our case, is too low to capture such dynamics without aliasing according to the Nyquist–Shannon sampling theorem. Increasing the sampling frequency of the MPC to 200 Hz is unfavorable from the perspective of computational complexity. The higher frequency vibration is outside the frequency range of interest and has a limited impact on the aspect of comfort that this article focuses on. Thus, the radial dynamics of the tire is neglected. The OCP in the hybrid MPC is formulated as

$$
\begin{aligned}
\min_{F_{\text{act},*}} \quad & J_{\text{hyb}}(F_{\text{act},*}) \\
\text{s.t.} \quad & F_{\min} \leq F_{\text{act},*} \leq F_{\max}
\end{aligned}
\tag{10}
$$

where the cost function J_{hyb} is

$$
J = \sum_{i=1}^{k} q_z (z_* - z_{\text{ref},*})^2 + r_{\text{hyb}} F_{\text{act},*}^2.
\tag{11}
$$

The resemblance of the OCP in the hybrid MPC to the one in the NMPC is achieved by choosing the proper reference and weightings. The hybrid MPC controls the height of the sprung mass to follow a reference as

$$
\begin{aligned}
z_{\text{FL,ref}} &= z_{\text{RL,ref}} = \phi_{\text{ref}} \cdot B/2 \\
z_{\text{FR,ref}} &= z_{\text{RR,ref}} = -\phi_{\text{ref}} \cdot B/2.
\end{aligned}
\tag{12}
$$

If all four suspensions track their reference height, the vehicle body would consequently track the reference roll angle. The equivalence of weighting is given by

$$
\begin{aligned}
q_{z,\text{hyb}} \cdot z_{*,\text{ref}}^2 &= q_{\phi,\text{NMPC}} \cdot \phi_{\text{ref}}^2 \\
r_{\text{hyb}} \cdot F_{\text{act},*}^2 &= r_{\text{NMPC}} \cdot F_{\text{act},*}^2.
\end{aligned}
\tag{13}
$$

Given the identical penalty on the control effort in both OCPs, the penalty on height tracking error should equal the penalty on the consequent roll tracking error. The hybrid MPC is implemented using the Multiparametric Toolbox [28] and the OCP is solved on a uniform grid of the 3-D space of z_*,

TABLE II

COMPARISON OF ROLL AND PITCH MOMENT OF INERTIA

Moment of Inertia	Roll	Pitch
Rigid Body [kg m^2]	718.2	2783.8
4 Point Masses [kg m^2]	1020.1	3341.1
Difference [%]	42.0	20.0

$\dot{z}_*$, $z_{\text{ref},*}$ and the initial output is evaluated by linear interpolation (see Fig. 7). In total, the OCP is solved 3549 times. Using multiparametric optimization for generating the explicit control low would reduce the loss optimality than the grid approach but the computational time is observed to be too high even for offline processing. Instead, we expect online optimization to compensate for the loss of optimality.

Nevertheless, there are further fundamental differences when modeling a rigid body with four separate point masses. They should be carefully considered to avoid invalidating the initialization scheme. First, the four sprung masses do not yield precisely the actual moment of inertia of roll and pitch when connected with rigid links. The comparison is given in Table II. The mismatch in moments of inertia may cause the hybrid MPC to demand a larger force than the actual optimal force according to the NMPC's OCP. Moreover, the quarter-car models alone can by no means capture the load transfer caused by planar accelerations. The load transfer influences each individual quarter-car model as an external disturbance and should be compensated for with

$$F_{\text{comp},*} = m_s a_y (h_{\text{cg}} - h_{\text{cr}})/(2B) \cdot s_{\text{side}}$$
$$s_{\text{side}} = \begin{cases} 1, * \in \{\text{FR,RR}\} \\ -1, * \in \{\text{FL,RL}\}. \end{cases} \tag{14}$$

The compensatory component is added to the initial output by interpolating the hybrid OCP solutions to eventually construct the starting point as

$$F_{\text{act},*}^{\text{init}} = F_{\text{interp},*} + F_{\text{comp},*}. \tag{15}$$

The eventual starting point is expected to reduce the online computational load and to serve as a valid control input by itself. Relevant results will be presented in Section IV.

E. Nonlinear Programming Solver

From the starting point determined as described above, local optimization is further performed to find the optimal control input. We implemented the gradient descent method with inexact (backtracking) line search [29]. To incorporate the constraints on control inputs, a shrinkage of the step length also happens when the current step size causes a violation. The algorithm stops when the norm of the local gradient is below a certain threshold, or when the number of iterations exceeds a certain limit. The latter allows us to balance between the performance gain and the computational load, which can be exploited when running the controller with limited computational resources.

III. SIMULATION SETUP

The proposed control strategy is examined in a virtual environment in multiple scenarios. The simulation platform
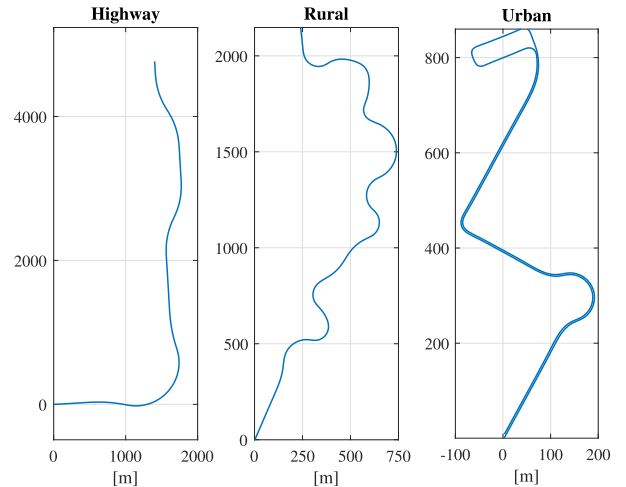

Fig. 8. Road profiles of the proposed scenarios for the simulation study.

is IPG CarMaker, in which a passenger car's dynamics is modeled in detail and experimentally validated by DRiV Incorporated, which includes validated sub-models of the active suspension actuators. A virtual driver model controls the vehicle's longitudinal and lateral motion to follow the desired route. It allows deviating from the lane center to reduce the curvature of the path and the velocity is regulated such that the acceleration stays within a predefined envelope. In the simulation, the velocity-dependent curvature preview is implemented with a virtual road sensor, while in reality this may be enabled by high-precision road maps and/or the environmental perception systems on automated vehicles. The simulation is initially executed on a desktop PC (3.7-GHz Hexa-core CPU plus 64-GB DDR4 RAM) for understanding the behavior of the system and tuning the parameters before moving to a hard real-time platform (see details in Section III-C).

A. Scenarios

The system is supposed to operate on well-paved roads only. We adopted three typical scenarios that are commonly experienced in daily driving, namely, the highway, rural, and urban scenarios. Highway driving mainly features sustained cornering motion that changes gradually and the peak magnitude of the acceleration is rather low, too. The longitudinal velocity would stay mostly constant. This scenario mainly tests the system's performance in terms of steady-state tracking. Driving in urban areas is the exact opposite as it involves sharp turnings with shorter duration and moderate magnitude, in addition to the frequent changing of direction and speed. It examines the system's dynamic response to quick-changing reference. In between is the rural scenario where mid- to high-speed corners are common. The corners can be closely adjacent to each other and the curvature varies continuously. A higher magnitude of lateral acceleration than the other scenarios may be observed. The paths of the vehicle in the proposed scenarios are shown in Fig. 8.

B. Evaluation

The simulation study aims to evaluate the proposed system from two perspectives: control quality and motion comfort. For
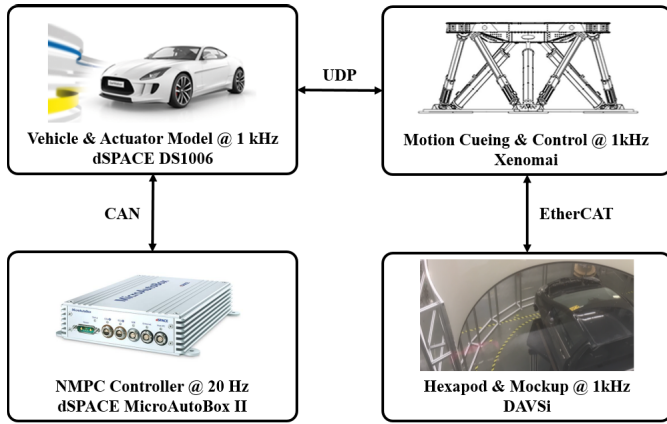
Fig. 9. Schematic drawing of the HIL experiment setup explaining the functions of each platform and the communications between the platforms.
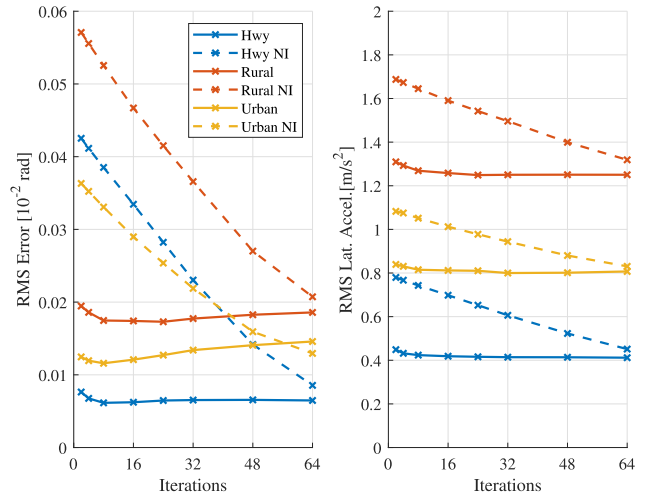

Fig. 10. Variation in the comfort and control performance indicators when different numbers of iterations in the nonlinear optimization are performed. The term NI in the legends stands for "no initialization," meaning the optimization process starts from zeros.

control quality, we focus on the tracking error of the roll angle, specifically, the root-mean-square (RMS) value of the error signal. Motion comfort, on the other hand, is a more comprehensive quality to quantify and measure. Extensive guidelines of comfort evaluation subject to mechanical vibrations can be found in ISO 2631-1. However, the proposed method only aims to reduce the lateral acceleration exerted on the occupant to mitigate motion sickness. Thus, we adopt the frequency weighting proposed in [30] for motion sickness induced by lateral oscillations. A virtual inertial measurement unit (IMU) is placed at the approximate position of the otolith organs of the occupant. The IMU's orientation is fixed to the vehicle body, assuming that the occupant is relevantly static to the vehicle. In addition to examining the RMS value of the sensed lateral acceleration, we further take into account the human body's sensitivity to vibrations with different frequencies. The lateral acceleration signal's power distribution (PSD) is calculated first before the aforementioned weighting is applied. To help demonstrate the performance of the NMPC method, we also included a PID-based curve tilting controller as the baseline. The PID controller is accompanied by the same disturbance compensating input as a feed-forward term that counteracts lateral load transfer. The PID output is bounded according to the actuators' capability and its integral component resets to zero once the reference roll angle starts to change. This helps combat the windup issue due to the relatively large integral gain. The PID controller is tuned per scenario to maximize its performance while the weighting parameters in the NMPC remain constant. Additional simulation runs are performed using the output of the explicit initialization as control input such that the validity of the initialization scheme is verified.

C. HIL Setup

To further validate whether the control method is efficient enough for real-time implementation with limited computational resources, the simulation runs have been repeated on an HIL setup (see Fig. 9). The controller is compiled on a dSPACE MicroAutoBox II, which carries a single-core 900-MHz processor and 16-MB random memory. This device has been widely used in the industry to test proto-

type control algorithms. It yields a feasible performance for industrial microprocessors targeting highly automated vehicles (e.g., the quad-core 800-MHz NXP S32S247). The simulation environment is compiled on the dSPACE DS1006 processing board (quad-core 2.8-GHz CPU, 1-GB DDR2 RAM). The two devices communicate via a CAN bus, on which the virtual vehicle exchanges the controller's command with the necessary measurements. The communication operates at 20 Hz, identical to the controller's sampling frequency, while the vehicle dynamics are updated at 1 kHz. Also included in the HIL setup is the Delft Advanced Driving Simulator (DAVSi) [31], which mainly consists of a mock-up of the front half of a Toyota Yaris and a hexapod motion platform driven by six linear motors. The experiment runs in hard real-time mode, where if the turnaround time of the controller exceeds the sampling time, the simulation is terminated immediately.

IV. RESULTS AND DISCUSSION

A. Numerical Performance

The NMPC's solver settings influence the trade-off between computational effort and performance. The key parameter in our case is the number of iterations. This parameter is varied between 2 and 64. The corresponding performance indicators are shown in Fig. 10. The contribution of the initialization scheme is apparent. After a small number of iterations, the tracking error and the resultant lateral acceleration do not decrease steeply anymore. Performing more iterations is not significantly beneficial especially when considering the limited computational resource for real-time implementation. In the more dynamic scenarios, the tracking error starts to grow at a larger number of iterations. This is partly due to the assumption that the disturbances are constant throughout the prediction horizon whose validity diminishes in this scenario. Another part of the contribution comes from the potential model mismatch. It is nevertheless challenging to formulate a compact prediction model to capture all the
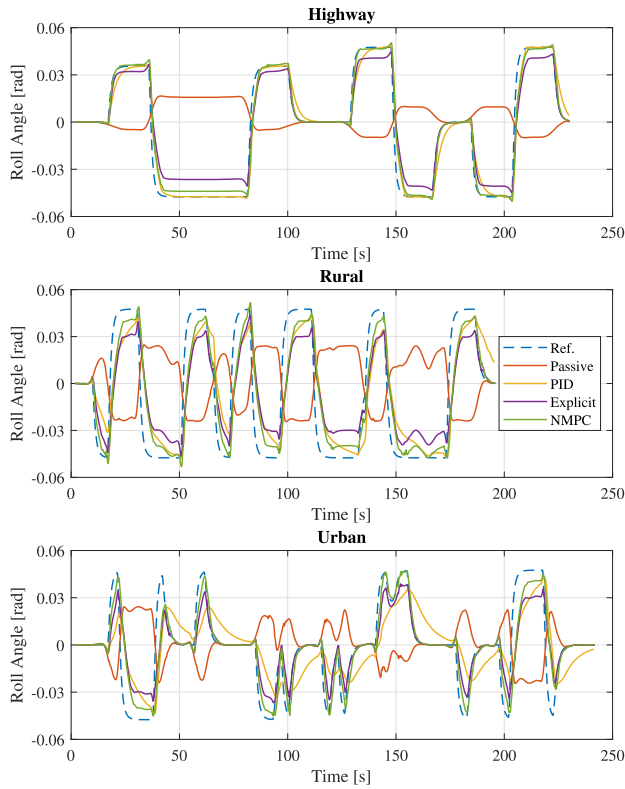
Fig. 11.   Roll angles of the vehicle body per simulation scenario. In each sub-graph, the roll angles of a vehicle with passive suspension and with active suspension using different methods are compared against the reference value.

TABLE III
COMPARISON OF THE TRACKING PERFORMANCE OF THE CONTROL METHODS USED IN SIMULATION

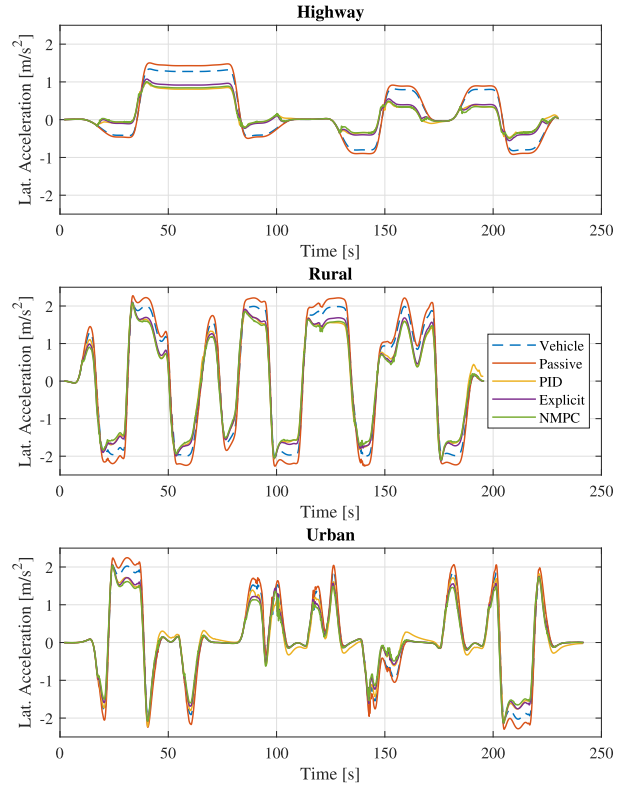| Controller	Tracking Error	Highway	Rural	Urban
PID	RMS [10^{-2} rad]	0.706	2.090	1.868
Explicit	RMS [10^{-2} rad]	0.881	2.053	1.330
	Difference [%]	+24.8	-1.8	-28.8
NMPC	RMS [10^{-2} rad]	0.615	1.747	1.159
	Difference [%]	-12.9	-16.4	-38.0

Fig. 12.   Lateral accelerations per simulation scenario. In each sub-graph, the lateral acceleration exerted on the occupants on a vehicle with passive suspension and with active suspension using different methods is compared against the lateral acceleration of the vehicle body.

complex multibody dynamics of a passenger vehicle. Because the equivalent moments of inertia in the initialization scheme are higher, the starting point of the optimization is likely to yield a higher control effort. This is on some occasions helpful in reducing the tracking error. By further optimizing the control inputs, the control effort would decrease while allowing marginally larger tracking error. The trend is different when the NMPC solver starts from all zeros, where both indicators keep decreasing up to 64 iterations. Though a comparable performance level is only achieved at 64 iterations, illustrating the contribution of the initialization scheme. Eventually, eight iterations are chosen for further analysis. With this setting, a worst case turnaround time of 43 ms has been observed in the HIL experiment. This is lower than the sampling time of the controller, 50 ms, proving that the proposed NMPC controller is capable of real-time implementation.

B. Control Quality

The simulation results for the three scenarios in terms of roll tracking are shown in Fig. 11. The RMS tracking error per control method per scenario is compared in Table III. In the highway scenario, the reference roll angle stays constant for long periods of time, allowing the integral action of PID to correct the error. The model-based approaches, i.e., the explicit control and NMPC, yield a constant tracking error due to potential model mismatch. This disadvantage becomes less obvious in rural and urban scenarios, where the reference roll angle varies more frequently. The integral action is not given

sufficient time to bring down the error before the reference value changes. The quicker response of explicit control and NMPC contributes in these situations to the reduction of the error, demonstrating the superiority of the prediction over the reaction in a more dynamic environment. These two methods show minor non-minimum-phase behavior at the beginning of a changed reference, though. Because when the vehicle leaves a steady-state cornering motion, the assumption of constant lateral acceleration through the prediction horizon does not hold. The actual lateral acceleration experienced by the vehicle is lower than what the controller expects. Hence, the controller commands a larger force than the actual need.

C. Motion Comfort

The lateral acceleration sensed by the occupants is shown in Fig. 12, indicating their level of discomfort. Table IV compares the lateral acceleration sensed by the occupant, with and without the curve tilting function and using different
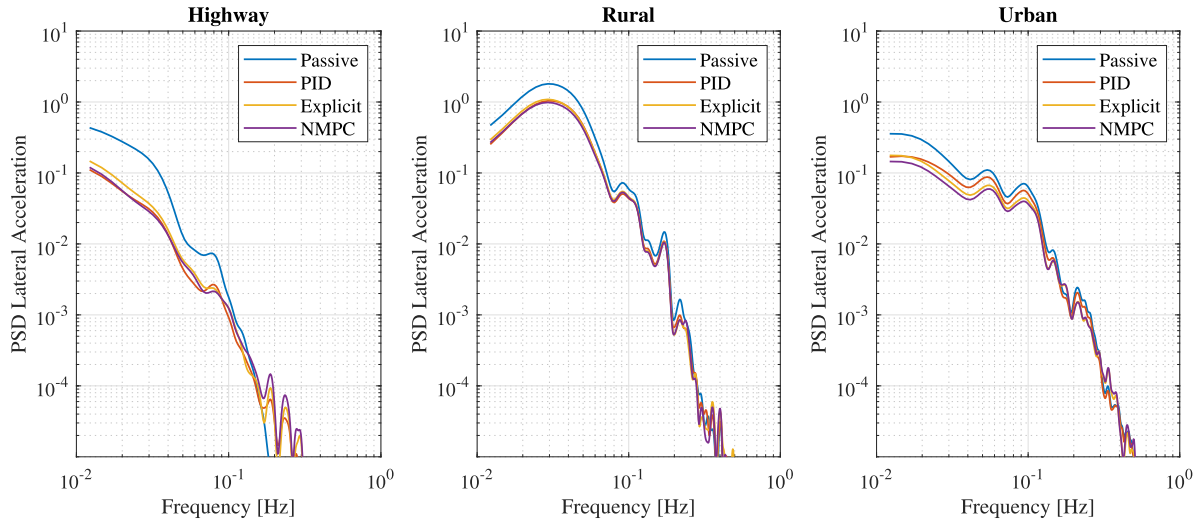
Fig. 13. Frequency-domain power distribution of the lateral acceleration sensed by the occupant.

TABLE IV

COMPARISON OF THE MOTION COMFORT IN TERMS OF RMS LATERAL ACCELERATION USING DIFFERENT CONTROL METHODS USED IN SIMULATION

Controller	Acceleration	Highway	Rural	Urban
Passive	RMS [$\mathrm{m\,s^{-2}}$]	0.796	1.710	1.103
PID	RMS [$\mathrm{m\,s^{-2}}$]	0.414	1.300	0.882
	Difference [%]	-47.8	-23.6	-19.3
Explicit	RMS [$\mathrm{m\,s^{-2}}$]	0.465	1.326	0.856
	Difference [%]	-41.3	-22.1	-21.7
NMPC	RMS [$\mathrm{m\,s^{-2}}$]	0.424	1.269	0.815
	Difference [%]	-46.5	-25.4	-25.4

control methods. The body of a passive vehicle leans away from the curvature center when cornering, slightly magnifying the lateral acceleration on the occupant. The effectiveness of the tilting functionality is significant in the highway scenario where all control methods achieved a reduction in lateral acceleration by 40%. In rural and urban scenarios, the benefit of the system decreases to the range of 20%–25% due to multiple reasons. On one hand, the absolute magnitude of the reduction in lateral acceleration is limited by the roll angle available. The same amount of reduction becomes less obvious on a relative scale when the actual magnitude is larger. On the other hand, the system is not able to respond sharply to the highly dynamic planar motion. The roll velocity is penalized to ensure a gentle transition and avoid introducing another source of discomfort. Even the predictive control methods are only reacting to a change in reference. Though according to the RMS acceleration the advantage of using NMPC over PID is only marginal, in contrast to the more visible improvement in terms of tracking accuracy. This is primarily because the RMS value is more sensitive to the higher amplitude part of the signal. The higher amplitude is usually coupled with steady-state tracking of saturated reference roll angle, which is a result of limited roll angle allowed by the suspension geometry. NMPC outperforms PID mainly in transient response when the actual lateral acceleration is relatively low. The

phase lead of the reference generator also helps mitigate the negative impact of the PID's slower response on the resulted comfort quality. Nevertheless, the trend is consistent between Tables III and IV that NMPC's advantage over PID is more obvious in more dynamic driving scenarios. In addition to the RMS value of the sensed acceleration, we further analyzed the signal's property in the frequency domain. The power spectral density is computed and weighted according to the recommendations in [30], which indicates a higher influence in the low-frequency range up to 0.25 Hz. The resulting weighted PSDs are displayed in Fig. 13. With the actively controlled roll motion, a significant improvement is observed in the frequency range of up to approximately 0.1 Hz in all three scenarios. Though the active control on the roll motion slightly elevates the high-frequency components in the highway scenario where the passive motion is steady.

V. CONCLUSION

A. Contributions

This article presents an NMPC strategy for the curve tilting functionality using active suspensions. The application mainly aims to exploit the full potential of the concept on automated passenger vehicles in the future, where the predictive feature of the NMPC can be joined by the motion planning algorithm. To tackle the commonly reported challenge of reducing the computational load for solving the OCP online, we proposed an explicit initialization scheme. By precomputing a lookup table offline, the starting point of the nonlinear optimization is quickly determined by 3-D linear interpolation. The lookup table results from a hybrid modeling method of the quarter-car dynamics with highly nonlinear suspension forces. Based on this model, a hybrid MPC problem has been formulated, reflecting the same objectives and weightings as in the NMPC. The alternative OCP is solved on a wide range of initial and reference states to form a lookup table. The output of the interpolation is further combined with disturbance compensation, which estimates and counteracts the influences of load

transfer that are not captured by the quarter-car model. The eventual starting point is supposed to yield a valid control input. Simulation shows that controlling the suspensions with the initialization scheme already enables the desired functionality. Further performing the online optimization in NMPC improves the transient response and reduces the tracking error. The NMPC approach yields a better overall tracking performance in all three driving scenarios (12.9%, 16.4%, and 38.0% smaller, respectively) albeit being slightly outperformed by PID in steady-state tracking where the integral action is highly beneficial. HIL experiment on limited computational resources confirms the real-time capability of the proposed method, whose parameters are chosen to balance the additional computational effort and the marginal performance gain. Also, thanks to the explicit initialization scheme, the NMPC solver's computational load is reduced significantly compared with starting the optimization from zeros.

B. Limitations and Future Works

The current study shows certain disadvantages. Neglecting the dynamics of the unsprung masses implies that the performance may not be as satisfactory when driving on a rough road. Nevertheless, the major source of discomfort under such circumstances would be the vertical excitation instead of the lateral acceleration. The HIL simulation reveals that the full capability of the NMPC scheme is not yet fully realized with the hardware available to us. The computational capability of the HIL hardware, released in 2010, is not representative of what could be available on the latest highly automated vehicles, given the rapid development in high-performance automotive microcontrollers. It is interesting to investigate whether the numerical efficiency could be boosted with parallel computing on multi-core microcontrollers. For industrial applications, the code would be further optimized for efficiency and could run faster than in the rapid-prototyping phase. Such advances may allow a more complex prediction model in the NMPC although the model validation process would become more challenging, too. Another limitation of the article is that the comfort aspects are only measured with arbitrary indicators. In the future, we plan to perform subjective comfort studies using an experimental vehicle. The latter also allows to fine-tune the vehicle's tilting behavior and helps validate the control quality of the proposed method. Finally, the current system would be combined with a comfort-oriented motion planning algorithm. It enables a more accurate estimation of the disturbances from the planar motion and the optimal generation of reference roll motion.

REFERENCES

[1] M. Kyriakidis, R. Happee, and J. C. F. de Winter, "Public opinion on automated driving: Results of an international questionnaire among 5000 respondents," *Transp. Res. F, Traffic Psychol. Behav.*, vol. 32, pp. 127–140, Jul. 2015.

[2] M. J. Griffin and M. M. Newman, "Visual field effects on motion sickness in cars," *Aviation, Space, Environ. Med.*, vol. 75, no. 9, pp. 739–748, 2004.

[3] P. Matsangas, M. E. McCauley, and W. Becker, "The effect of mild motion sickness and sopite syndrome on multitasking cognitive performance," *Hum. Factors, J. Hum. Factors Ergonom. Soc.*, vol. 56, no. 6, pp. 1124–1135, Sep. 2014.

[4] P. S. Els, N. J. Theron, P. E. Uys, and M. J. Thoresson, "The ride comfort vs. handling compromise for off-road vehicles," *J. Terramech.*, vol. 44, no. 4, pp. 303–317, Oct. 2007.

[5] C. Poussot-Vassal, C. Spelta, O. Sename, S. M. Savaresi, and L. Dugard, "Survey and performance evaluation on some automotive semi-active suspension control methods: A comparative study on a single-corner model," *Annu. Rev. Control*, vol. 36, no. 1, pp. 148–160, Apr. 2012.

[6] H. E. Tseng and D. Hrovat, "State of the art survey: Active and semi-active suspension control," *Vehicle Syst. Dyn.*, vol. 53, no. 7, pp. 1034–1062, 2015.

[7] C. M. Oman, "Sensory conflict in motion sickness: An observer theory approach," *Pictorial Commun. Virtual Real Environ.*, pp. 362–376, 1991.

[8] M. Bär, *Vorausschauende Fahrwerkregelung zur Reduktion Der Auf Die Insassen wirkenden Querbeschleunigung*. Forschungsges, Munich, Germany: Kraftfahrwesen (fka), 2014.

[9] H. R. Harris, E. Schmid, and R. A. Smith, "Introduction: Theory of tilting train behaviour," *Proc. Inst. Mech. Eng., F, J. Rail Rapid Transit*, vol. 212, no. 1, pp. 1–5, Jan. 1998.

[10] S. Cytrynski, U. Neerpasch, R. Bellmann, and B. Danner, "The active suspension of the new mercedes-benz GLE," *ATZ worldwide*, vol. 120, no. 12, pp. 42–45, Dec. 2018.

[11] D. Milakis, B. Van Arem, and B. van Wee, "Policy and society related implications of automated driving: A review of literature and directions for future research," *J. Intell. Transp. Syst. Technol. Planning, Oper.*, vol. 21, no. 4, pp. 324–348, 2017.

[12] D. Boocock and B. L. King, "The development of the prototype advanced passenger train," in *Proc. Inst. Mech. Eng.*, vol. 196. no. 1, Jun. 1982, pp. 35–46.

[13] T. Pilutti and A. G. Ulsoy, "Identification of driver state for lane-keeping tasks," *IEEE Trans. Syst., Man, Cybern. A, Syst. Humans*, vol. 29, no. 5, pp. 486–502, Sep. 1999.

[14] F. Borrelli, P. Falcone, T. Keviczky, J. Asgari, and D. Hrovat, "MPC-based approach to active steering for autonomous vehicle systems," *Int. J. Veh. Auton. Syst.*, vol. 3, nos. 2–4, pp. 265–291, 2005.

[15] E. Siampis, E. Velenis, S. Gariuolo, and S. Longo, "A real-time nonlinear model predictive control strategy for stabilization of an electric vehicle at the limits of handling," *IEEE Trans. Control Syst. Technol.*, vol. 26, no. 6, pp. 1982–1994, Nov. 2017.

[16] M. Diehl, H. G. Bock, and J. P. Schlöder, "A real-time iteration scheme for nonlinear optimization in optimal feedback control," *SIAM J. Control Optim.*, vol. 43, no. 5, pp. 1714–1736, Jul. 2005.

[17] M. N. Zeilinger, C. N. Jones, and M. Morari, "Real-time suboptimal model predictive control using a combination of explicit MPC and online optimization," *IEEE Trans. Autom. Control*, vol. 56, no. 7, pp. 1524–1534, Jul. 2011.

[18] M. Schulze Darup and M. Monnigmann, "Explicit feasible initialization for nonlinear MPC with guaranteed stability," in *Proc. IEEE Conf. Decis. Control Eur. Control Conf.*, Dec. 2011, pp. 2674–2679.

[19] Y. Zheng and B. Shyrokau, "A real-time nonlinear MPC for extreme lateral stabilization of passenger vehicles," in *Proc. IEEE Int. Conf. Mechtron. (ICM)*, Mar. 2019, pp. 519–524.

[20] M. Kissai, B. Monsuez, X. Mouton, D. Martinez, and A. Tapus, "Adaptive robust vehicle motion control for future over-actuated vehicles," *Machines*, vol. 7, no. 2, p. 26, Apr. 2019.

[21] S. Ikenaga, F. L. Lewis, J. Campos, and L. Davis, "Active suspension control of ground vehicle based on a full-vehicle model," in *Proc. Amer. Control Conf. (ACC)*, vol. 6, Jun. 2000, pp. 4019–4024.

[22] M. Zapateiro, F. Pozo, H. R. Karimi, and N. Luo, "Semiactive control methodologies for suspension control with magnetorheological dampers," *IEEE/ASME Trans. Mechatronics*, vol. 17, no. 2, pp. 370–380, Apr. 2012.

[23] W. F. Milliken and D. L. Milliken, *Race Car Vehicle Dynamics*, vol. 400. Warrendale, PA, USA: Society of Automotive Engineers, 1995

[24] W. P. M. H. Heemels, B. De Schutter, and A. Bemporad, "Equivalence of hybrid dynamical models," *Automatica*, vol. 37, no. 7, pp. 1085–1091, 2001.

[25] A. Bemporad, D. Mignone, and M. Morari, "An efficient branch and bound algorithm for state estimation and control of hybrid systems," in *Proc. Eur. Control Conf. (ECC)*, Aug. 1999, pp. 557–562.

[26] D. Axehill and M. Morari, "Improved complexity analysis of branch and bound for hybrid MPC," in *Proc. 49th IEEE Conf. Decis. Control (CDC)*, Dec. 2010, pp. 4216–4222.

[27] L. H. Yam, D. H. Guan, and A. Q. Zhang, "Three-dimensional mode shapes of a tire using experimental modal analysis," *Exp. Mech.*, vol. 40, no. 4, pp. 369–375, Dec. 2000.

[28] M. Herceg, M. Kvasnica, C. N. Jones, and M. Morari, "Multi-parametric toolbox 3.0," in *Proc. Eur. Control Conf. (ECC)*, Jul. 2013, pp. 502–510.

[29] L. Armijo, "Minimization of functions having Lipschitz continuous first partial derivatives," *Pacific J. Math.*, vol. 16, pp. 1–3, Nov. 1966.

[30] B. E. Donohew and M. J. Griffin, "Motion sickness: Effect of the frequency of lateral oscillation," *Aviation, Space, Environ. Med.*, vol. 75, no. 8, pp. 649–656, 2004.

[31] Y. R. Khusro, Y. Zheng, M. Grottoli, and B. Shyrokau, "MPC-based motion-cueing algorithm for a 6-DOF driving simulator with actuator constraints," *Vehicles*, vol. 2, no. 4, pp. 625–647, Dec. 2020.

Yanggu Zheng received the B.Sc. degree in automotive engineering from Tsinghua University, Beijing, China, in 2015, and the M.Sc. degree *(cum laude)* from Delft University of Technology, Delft, The Netherlands, in 2018, where he is currently pursuing the Ph.D. degree with the Department of Cognitive Robotics, Section of Intelligent Vehicles.

His research interests include the application of optimization-based control and motion planning methods on automated vehicles for safety and comfort.

Barys Shyrokau received the Dipl.Eng. degree *(cum laude)* in mechanical engineering from Belarusian National Technical University, Minsk, Belarus, in 2004, and the joint Ph.D. degree in control engineering from Nanyang Technological University, Singapore, and Technical University Munich, Munich, Germany, in 2015.

He is currently an Assistant Professor with the Department of Cognitive Robotics, Section of Intelligent Vehicles, Delft University of Technology, Delft, The Netherlands, and involved in research related to vehicle dynamics and control, motion comfort, and driving simulator technology.

Dr. Shyrokau is also the Scholarship and Award Holder of Fédération Internationale des Sociétés d'Ingénieurs des Techniques de l'Automobile (FISITA), Deutscher Akademischer Austauschdienst (DAAD), Singapore International Graduate Award (SINGA), International Society for Terrain-Vehicle Systems (ISTVS), and CADLM.
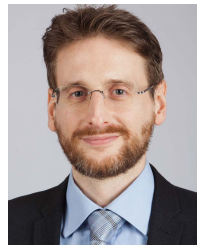
Tamás Keviczky (Senior Member, IEEE) received the M.Sc. degree in electrical engineering from Budapest University of Technology and Economics, Budapest, Hungary, in 2001, and the Ph.D. degree from the Control Science and Dynamical Systems Center, University of Minnesota, Minneapolis, MN, USA, in 2005.

He was a Post-Doctoral Scholar of control and dynamical systems with California Institute of Technology, Pasadena, CA, USA. He is currently a Professor with Delft Center for Systems and Control, Delft University of Technology, Delft, The Netherlands. His research interests include distributed optimization and optimal control, model predictive control, embedded optimization-based control and estimation of large-scale systems with applications in aerospace, automotive, mobile robotics, industrial processes, and infrastructure systems, such as water, heat, and power networks.

Dr. Keviczky was a co-recipient of the AACC O. Hugo Schuck Best Paper Award for Practice in 2005. He has served as an Associate Editor for *Automatica* from 2011 to 2017.

Monzer Al Sakka studied electrical and control systems engineering from the Université de Technologie de Belfort-Montbéliard (UTBM), Belfort, France, and received the M.Sc. degree in mechatronics from UTBM in 2006, and the dual Ph.D. degree in electrical engineering from UTBM and Vrije Universiteit Brussel (VUB), Ixelles, Belgium, in 2010.

Afterward, he worked as a Researcher with the Clean Powertrains Department, Flanders' DRIVE, Lommel, Belgium. He is currently a Senior Principal Engineer with Tenneco/DRiV, Sint-Truiden, Belgium. His research interests include electric/hybrid vehicles, power electronics, dc/dc converters, inductive charging, and electrical and thermal modeling of energy storage systems. His work consists of modeling, simulation, control, development, and implementation of automotive advanced suspension systems.

Miguel Dhaens received the M.Sc.Eng. degree in electro-mechanical engineering from KIH, Ostend, Belgium, in 1993 (associated with Catholic University of Leuven, Leuven, Belgium).

He is currently an Engineering Manager of the Global Research Ride Performance Team of Tenneco and responsible for defining the research road map and coordinating the global research activities of Tenneco's Ride Performance business, which includes vehicle dynamics (advanced sensing, autonomy, and emotional intelligence), damping solutions, mechatronics, material science, manufacturing technologies, and predictive tools. In this role, he chairs a team of 11 engineers and eight Ph.D. scientists and liaises with universities and knowledge centers. Before joining Tenneco, he worked as a Research and Development Manager with Flanders' DRIVE, Lommel, Belgium, and before that, he was a Manager for the engine race team and the test team and advanced strategies with Toyota Motorsport GmbH, Köln, Germany, in the Formula One (F1) Project. He started his career as a Project Engineer with Ilmor Engineering Ltd., Northampton, U.K., working in F1 and with Champ Car engines.